New Horizons in Structural Biology of Membrane Proteins

Subjects: Biochemistry & Molecular Biology | Biophysics | Biochemical Research Methods
Contributor: Olga Vinogradova , Robbins Puthenveetil ,

A third of both pro- and eukaryotic proteomes consist of membrane proteins. Housed in a milieu of hydrophobic molecules, they serve as crucial contacts of communication between the cytoplasm and non-cytosolic environments, making them essential pharmaceutical targets. While membrane proteins are notoriously difficult to investigate at any level, high-resolution structures of these targets only became feasible at the very end of the twentieth century. It was not until robust technological developments in the fields of X-ray crystallography, NMR spectroscopy and cryo-EM, that the scientific community at large, finally gained access to an ever-increasing number of atomic resolution structures, and began to rationalize how membrane proteins accommodate their function. As if the lack of structural information wasn't enough to hamper progress, a higher level of complexity arose from the modern understanding of "one structure—one function" paradigm, a primitive simplification useful at the dawn of the scientific era, that has promptly lost credence to the complex maneuvers of membrane proteins.

membrane proteins nuclear magnetic resonance

2. Nuclear Magnetic Resonance

Solution NMR (nuclear magnetic resonance) is one of the high-resolution techniques which allows for the investigation of both structural and dynamic properties of biological macromolecules. Being a solution technique, in contrast to X-ray crystallography or cryo-EM, NMR can be performed in environments that closely resemble native cellular conditions. Studying GPCRs, ion channels or transporters, etc., even in the best reconstitution media (reviewed in [1]) with the most advanced TROSY (transverse relaxation-optimized spectroscopy)-based methods [2], still requires perdeuteration and often does not provide desirable resolution and/or sensitivity. Fortunately, with the growing number of crystal/cryo-EM structures in the Protein Data Bank (PDB), researchers now have a detailed perspective on certain conformers, correlated with specific binding modes or activation states, for many intriguing targets. These atomic resolution structures offer the luxury to focus on specific sites within the protein most sensitive to conformational changes using molecular labels. Although this could be achieved by ^{1}H-^{13}C methyl TROSY analysis (reviewed in [3]) in deuterated samples, the easiest way is to employ ^{19}F NMR.

Several favorable nuclear spin properties of fluorine-19 (^{19}F), that have been exploited since the early days [4] are finding stronger footholds again. These include:

- High magnetic sensitivity: the ^{19}F isotope, in contrast to proton (^{1}H), the gold standard, has a high relative sensitivity of ~83% and a 100% natural abundance (note that relative sensitivity for detection in NMR

experiments at a constant number of nuclei is roughly proportional to the cube of their gyromagnetic ratios [5], $(\gamma_{F19}/\gamma_{H1})^3 = 0.94^3 = 0.83$).
- The lack of endogenous fluorine and thereby the absence of a background signal.

- Sensitivity to local environment: ^{19}F exhibits large chemical shifts dispersion (CSD) which spans 2000 ppm in comparison to a meager 13 ppm for ^{1}H; although chemical shifts, arising solely from local van der Waals electrostatic and solvent interactions, typically vary between 2.5 (CF_3) and 20 ppms (mono-fluoro-aromatics) [6], they may still be enough to characterize motional and structural properties of IMPs in different environments such as lipid vesicles, detergents or organic solvents.

- 1D spectroscopy, used to avoid unfavorable relaxation associated with multidimensional NMR methods, is usually sufficient for the separation of the peaks in ^{19}F spectrum and works even for potentially dynamic states that are characterized by broad lines. Thus, different states can be resolved, and their corresponding population quantified.

- Lastly, the lack of protein deuteration significantly improves the ease and efficacy of sample preparations.

The above advantages do come at a price. Assigning ^{19}F resonances to structural states is anything but trivial and often requires prior hints from other techniques. For the thoroughly studied GPCR family (reviewed in [7]), the assignments rely on population shifts in response to agonists vs. antagonists or reverse agonists binding. In an impressive study from the Prosser lab [8], five key functional states of adenosine A_{2A} receptor ($A_{2A}R$) complexed with hetero-trimeric G protein ($G\alpha_s\beta_1\gamma_2$), were characterized in phospholipid nanodisc using ^{19}F-NMR. Signal transduction was modeled using rigidity-transmission allostery (RTA) algorithms [9]; and $A_{2A}R$ conformational ensembles, corresponding to the above functional states, were visualized through the dynamic energy landscapes reflecting, activation, G protein coupling, and nucleotide exchange.

Alternatively, differences in paramagnetic relaxation enhancement (PRE) can be used for assigning ^{19}F resonances to structural states [10], but only when different conformations, feature distinct solvent exposures for the ^{19}F probe. In another novel approach, ^{19}F longitudinal relaxation rates (R1) and their distance-dependent enhancement by paramagnetic ions (Ni^{2+} chelated through di-histidine motif) were measured with the goal to assign resonances to different structural states. This estimated the rates of the conformational exchange for a model membrane transporter—Glt_{Ph}, aspartate/sodium symporter from *Pyrococcus horikoshii* [11].

The inter-conversion between different conformational states, occurring on a µs to ms time scale can be evaluated by Carr–Purcell–MeiBoom–Gill (CPMG) relaxation dispersion experiments [12]. This technique has been widely used to study dynamics and folding pathways in soluble proteins, for instance, to define “invisible” sparsely populated states [13]. In general, this method is not easily applicable to IMP/membrane-mimetic complexes of large molecular weight due to unfavorable relaxation rates in ^{1}H-based multidimensional NMR experiments. The ^{19}F-1D versions of these experiments, however, can be employed successfully to define exchange rates between GPCR states. For example, Manglik et al. showed that unliganded and inverse-agonist-bound β_2-adrenergic receptor

(β_2AR) predominantly existed in two inactive conformations that exchange within hundreds of µs. Agonists shifted the equilibrium towards a conformation capable of engaging cytoplasmic G proteins, although incompletely, resulting in an increased conformational heterogeneity with the coexistence of inactive, intermediate, and active states [14].

In another interesting approach, remarkable relaxation properties of the aromatic ^{13}C-F spin pair allowed for ^{19}F-^{13}C TROSY-based experiments, with direct detection from ^{13}C. The 2D spectra produced sensitive, high-resolution signals for a target, such as the single-ring α7 proteasome particle with an MW of 180 kDa [15], demonstrating the potential of solution NMR to study IMPs.

Incorporation of extrinsic ^{19}F-labels at relevant locations within the target protein is possible either through chemical conjugation of fluorine-containing small molecules with reactive amino acids or cysteine mutants, as was utilized in the above examples, or through biosynthetic introduction of fluorinated amino acid analogs [16][17]. An interesting example of the latter can be found in the study of β-arrestin-1, employing the unnatural amino acid (3,5-difluorotyrosine, F2Y) to define its V2Rpp bound (V2-vasopressin receptor carboxy-terminal phosphopeptide) conformation and dynamics [18]. As a result, a longstanding puzzle regarding the receptor's phospho-coding mechanism that dictates selective structural features directed by either desensitization of the receptor or initiation of arrestin's own signaling pathway was resolved. An elegant model was proposed which suggested that the phosphate-binding site on arrestin's surface was arranged in "a shape similar to the holes in a flute" with movements controlled by the phospho-receptor "fingers".

3. Cryo-Electron Microscopy

Cryo-EM (cryo-electron microscopy), the most recent addition to the structural biology toolkit, can provide near-atomic resolutions of macromolecular assemblies. The advent of direct electron detectors, corrections for beam-induced movement and specimen drift along with developments in other auxiliary methodologies, has made cryo-EM the method of choice for membrane proteins, especially those recalcitrant to crystallization [19]. In contrast to X-ray crystallography, which relies on structural uniformity within the crystal lattice, single-particle cryo-EM offers the opportunity to inspect an ensemble of conformational states for dynamic systems, such as ion channels or cell surface receptors, snap-frozen in a thin layer of vitrified ice. Therefore, the steady-state distribution of different conformers under various buffer conditions or ligand titrations can be observed, elucidating potential pathways involving conformational rearrangements.

Hite et al. showcase this approach, presenting numerous states occurring along the reaction cycle of Slo2.2, a Na^+-dependent K^+ channel [20]. Series of datasets collected from a Na^+ gradient concentration of 20–160 mM revealed an ensemble of closed structures with a minor population of an open conformer which increased with increasing concentration. In contrast, a data set collected at a high concentration of 300 mM showed predominantly open conformers. Comparison of the titration conformers with activity data implied that not all open channels conduct ions. Interestingly, no stable intermediate structure was observed, suggesting that the channel opens in a highly concerted, switch-like process. This example highlights the importance of capturing images of a large

enough number of single particles. By doing so, it becomes possible to define multiple sub-states within the major conformational states.

From a historic perspective, the first-ever structure of an ion channel determined by cryo-EM with high enough resolution to allow identification of sidechains was TRPV1, a polymodal signal detector channel which belongs to a transient receptor potential (TRP) family. Liao et al. characterized the unligated closed state [21] while, in a companion study, Cao et al. defined two open states (toxin or capsaicin bound) [22]. These studies revealed that TRPV1 opening is associated with major structural rearrangements in the outer pore, including the pore helix and selectivity filter, and pronounced dilation of a hydrophobic constriction at the lower gate, suggesting a dual gating mechanism. Several high-resolution cryo-EM structures of the TRP family channels, incorporated into different membrane mimetics later followed [23][24][25][26]. More recently, Zhang et al. produced an impressive compendium of 25 structures of TRPV1 by adding a pair of toxins and/or altering the cations and pH [27]. The structures provided a mechanistic insight into the extensive pharmacology of TRPV1 by visualizing alterations in the selectivity filter and gate correlating their allosteric couplings with disparate stimuli. Conformational dynamics in TRPV1 have been further studied by TIRF microscopy [28] as briefly discussed further below.

Though membrane protein structural biologists rejoice at sidestepping the near-Sisyphean task of generating well-ordered crystals, cryo-EM still requires astute biochemical preparation of target proteins. Exemplifying this case, Chen and colleagues used a multifaceted approach, including disulfide trapping, X-ray crystallography, and cryo-EM, to isolate an elusive “open-channel” state of the prototypical elevator-type transporter Glt_{Ph} [29]. Glt_{Ph} is an archaeal homolog of excitatory amino acid transporters (EAATs) which mediate uptake of glutamate and aspartate in neuronal and glial cells. The EAATs maintain a peculiar side hustle, in that they also function as chloride channels and this activity is not coupled to amino acid transport [30]. This ion channel activity has been observed since the mid-1990s but was not structurally rationalized even through scrupulous cryo-EM examination of a solution ensemble of homolog Glt_{Tk} [31].

In vitro elucidation of the molecular bases of mechanosensation presents unique technical challenges and hearing is perhaps, at the biophysical level, the least understood of the senses. No fewer than three studies over the past year were released which employ cryo-EM to resolve states of prestin, an essential component of the cochlear amplifier [32][33][34]. Prestin is a member of the solute carrier 26 (SLC26) anion transporter family and functions as the electromotive molecule of outer hair cells (OHCs) which amplify incident sound waves. The membrane-integral motor pulls the unenviable double-duty of sensitivity to both membrane potential and tension [35]. By varying the anions and including the inhibitor salicylate, a collection of prestin states were captured revealing the protein as a domain-swapped dimer with an elevator-like conformational cycle. The structures indicated that prestin can tune its in-membrane cross-sectional area and (supplemented by molecular dynamics [MD] simulations) also locally alter its surrounding bilayer thickness. The studies unshroud the elegant means by which an integral membrane protein transduces an electrochemical signal into mechanical work.

It is worth noting that despite the advances in cryoEM, high-resolution structural information from the flexible or dynamic parts of the protein remain elusive, a feature of prime relevance for single-pass IMPs. A recent remarkable

study of integrin $\alpha_5\beta_1$, in its apo and fibronectin bound forms, by Schumacher et al. [36] illustrates this point. The C-terminal portion of the receptor, including the flexible lower legs, transmembrane helices, and the cytoplasmic tails, remained unresolvable in cryoEM maps.

Observing long-lived, equilibrium structural states with cryo-EM is increasingly facile and, as with X-ray crystallography (described below), much effort is being spent on developing time-resolved variants to scrutinize short-lived intermediates. Sub-second time resolution has been primarily achieved in a rapid mixing step immediately prior to grid vitrification which can afford resolution of up to ~10 ms [37]. Rapid mixing is accomplished either through (i) a microfluidic setup prior to spraying the sample or (ii) spraying separate solutions directly onto a grid plunging into liquid ethane [38][39][40]. As a proof of concept for on-grid mixing, Dandey et al. observed large conformational shifts induced by rapidly mixing Ca^{2+} with MthK, a calcium-gated potassium channel which inactivates over the course of seconds [40]. Though the data were insufficient to clearly resolve an unseen open or intermediate MthK conformation, a time-resolved EM methodology by rapid mixing appears very feasible for membrane proteins with dynamics in the ms–s time scale.

The utility of cryo-EM is attested to by the burgeoning number of PDB depositions. New methodologies, however, must be cultivated for extracting dynamic structural information in the μs–ms regime where many protein motions lie. One attractive alternative strategy to microfluidic or on-grid mixing is flash photolysis of caged compounds to homogeneously initiate protein dynamism [41][42]. This approach was demonstrated using acid-sensing ion channel ASIC1a as a test subject, whereby protons were released from the photocaged sulfate MPNS to drop the solution pH and shift the channel from a resting state to desensitized.

4. Serial X-ray Crystallography

X-ray crystallography has historically been the gold standard for structure solutions with achievable resolutions occasionally extending below 1 Å. With improved detector speed and high photon flux at third-generation synchrotrons, time-resolved crystallography (TRX) became feasible in the 1990s. Though even with advanced facilities, a key difficulty to surmount in these experiments is homogeneous initiation of the reaction process, hence the targets typically studied are light-sensitive and can be triggered by a laser pulse. Many targets are, however, not light-sensitive but can be interrogated through clever application of photocaged substrates or shifts in temperature or pH. Another drawback of TRX is crystal packing itself which constrains protein conformation and may preclude some biologically relevant conformational changes. Nevertheless, the TRX approach is powerful in addressing ultrafast (fs–ps) motions as well as slower processes which do not grossly distort the protein and disrupt the crystal lattice.

TRX comprises two basic approaches: Laue diffraction methods on single large crystals and serial crystallography on many small crystals. The former relies on polychromatic (pink) X-ray beams and a full dataset can be collected using only a few diffraction frames, unlike with monochromatic X-rays. A primary weakness of Laue diffraction is, unfortunately, its intrinsic sensitivity to crystal mosaicity and stringent requirement for high-quality crystals. Serial

crystallography was pioneered by X-ray free-electron laser (XFEL) sources and subsequently has been adapted for synchrotron sources as well [43][44].

Integral membrane proteins tend to be more refractory toward crystallization and thus few have been investigated by Laue diffraction methods. Bacteriorhodopsin (bR) is a well-studied protein, with the advantageous trait of comprising a light-sensitive retinal prosthetic group, but even its crystals proved too fragile to withstand repeated pump-probing [45]. The lone success has been with the photosynthetic reaction center complex from *Blastochloris viridis* [46][47]. The first study revealed no discernable conformational change upon photoactivation (3.3 Å resolution model) while the second showed reorientation of a tyrosine close to the “special pair” (SP) bacteriochlorophylls at a higher resolution of 2.9 Å.

The more fruitful avenue for TRX thus far has been through serial crystallography. Serial femtosecond crystallography (SFX) was realized at XFEL sources over the past decade to accommodate for ultrahigh photon flux which obliterates exposed materials via Coulomb explosion. Useful data can be collected via what is colloquially known as “diffraction before destruction”, whereby single diffraction frames can be detected (presuming a diffracting crystal is in the beam path) [48]. Sample destruction obviously necessitates a comparatively large quantity of experimental mass but, in practice, this downside tends to result in other gains in efficiency. For instance, [sub]micron crystals are less tedious to produce but can diffract well especially from the high intensity of an XFEL. Additionally, with time-resolved studies, small crystal size affords less optical absorbance (i.e., for stimulating laser pulses) and rapid reactant diffusion, both of which improve reaction synchrony across a crystal.

As with (Laue) crystallography, soluble proteins tend to be better studied by TR-SFX but the technique has been exploited for a handful of (primarily light-sensitive) membrane proteins. Photosystem I, in complex with electron acceptor ferredoxin, provided the first test case by observing alterations in diffraction intensities using laser pulse-probing at 5 and 10 µs delays [49]. The collected data were not sufficient for high-resolution model building but verified the utility of pulse-probe methods ported from Laue crystallography to TR-SFX. Photosystem II (PSII) is thus far the most thoroughly examined membrane protein by TR-SFX [50][51][52][53][54][55][56][57][58][59][60]. Despite its name, PSII is the first protein in the photosynthetic chain and catalyzes light-driven water oxidation at the oxygen-evolving complex (OEC), a Mn_4CaO_5 cluster [61]. The reversible photocycle of PSII has been proposed to encompass five redox states, S_0–S_4, which evolve over a µs–ms timescale after photon absorption [62]. Most of the TR-SFX studies showed subtle or no conformational alteration, though, efforts were hampered by the achievable resolution. Later works have focused on the PSII OEC and have successfully produced snapshots of intermediate states with oxygen and water coordination, bringing closer a detailed mechanistic understanding of photosynthetic splitting of water.

The dynamics of the photosynthetic reaction center were recently followed up using ultrafast (i.e., picosecond timescale) TR-SFX [63]. Using pump-probe delays of 1 ps up to 8 µs, the authors captured photoactivated structural perturbations of the aforementioned SP chlorophylls which lead to low-amplitude oscillations within the protein to accommodate charge transfer and heat dissipation.

Rhodopsins have been highly studied for decades and, besides being convenient model proteins, have become important biotechnological tools for optogenetics and synthetic biology. The pigment retinal is the rhodopsins' essential cofactor which isomerizes upon photon absorption and induces conformational changes to elicit ion transport [64]. bR is, unsurprisingly, the model protein of choice and its dynamics have been probed from sub-picosecond through millisecond regimes [65][66][67]. The molecular movies derived through TR-SFX illuminate each step in the bR photocycle, directly visualizing retinal isomerization, side-chain reorientations, and backbone shifts which drive proton pumping (**Figure 1**). In addition, these structural data inform quantum mechanics/molecular mechanics (QM/MM) simulations and rationalize how the protein scaffold has been evolutionarily honed to optimize the retinal quantum yield. Subsequently, the maturing TR-SFX method was directed on rhodopsins KR2, ClR, and ChR to decipher the physicochemical origins of their differing substrate selectivities [68][69][70].

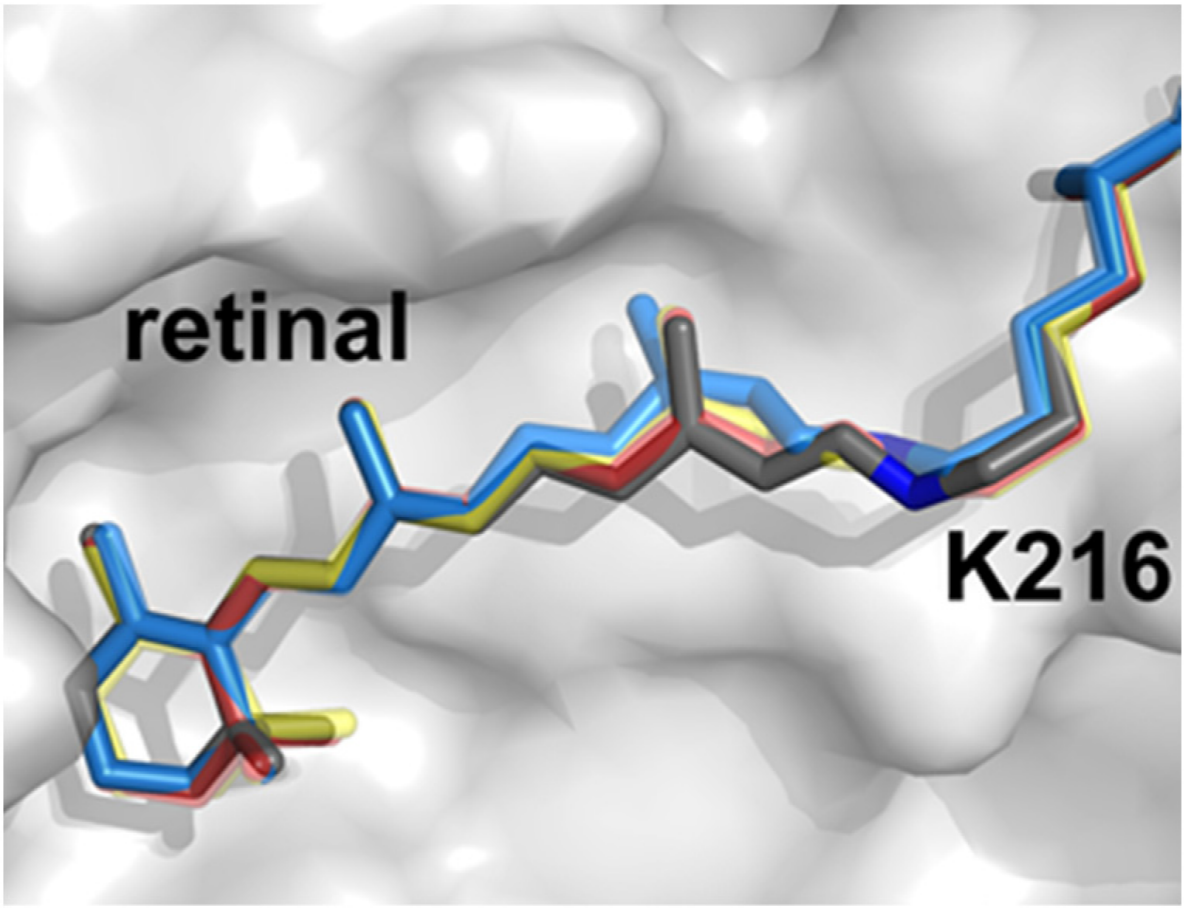

Figure 1. bR retinal *trans*-to-*cis* isomerization observed by ultrafast TR-SFX. Dark grey indicates the dark state, red and orange intermediates (49–406 and 457–646 fs), and blue the 13-*cis* isomer (10 ps) prior to relaxation. Illustration derived from PDB 6G7H, 6G7I, 6G7J, 6G7K.

Rounding out the membrane proteins subjected to TR-SFX is bovine cytochrome *c* oxidase (C*c*O) [71][72]. C*c*O catalyzes the reduction of dioxygen to two water molecules and is the terminal enzyme of the electron transfer chain in the inner mitochondrial membrane. To induce previously unseen intermediates, two studies used disparate stimuli: CO photolysis or rapid mixing with oxygen-saturated buffer. Both studies observed a similar oxidized heme

a_3 intermediate and, complemented with TR spectroscopy, gleaned new details on the enzyme's trafficking of electrons to effect unidirectional proton flux. These subjects highlight the strength of TR-SFX in resolving protein structural dynamism in the fs to ms timescale. User access to XFEL sources is, unfortunately, very limited but facilities are continuously innovating to increase their data acquisition and analysis capabilities [73].

References

1. Puthenveetil, R.; Vinogradova, O. Solution NMR: A powerful tool for structural and functional studies of membrane proteins in reconstituted environments. J. Biol. Chem. 2019, 294, 15914–15931.
2. Pervushin, K.; Riek, R.; Wider, G.; Wüthrich, K. Attenuated T2 relaxation by mutual cancellation of dipole-dipole coupling and chemical shift anisotropy indicates an avenue to NMR structures of very large biological macromolecules in solution. Proc. Natl. Acad. Sci. USA 1997, 94, 12366–12371.
3. Schutz, S.; Sprangers, R. Methyl TROSY spectroscopy: A versatile NMR approach to study challenging biological systems. Prog. Nucl. Magn. Reson. Spectrosc. 2020, 116, 56–84.
4. Mooney, E.F.; Winson, P.H. Fluorine-19 Nuclear Magnetic Resonance Spectroscopy. Annu. Rep. NMR Spectrosc. 1968, 1, 243–311.
5. Canet, D. NMR: Concepts and Methods; Wiley: New York, NY, USA, 1991.
6. Picard, L.P.; Prosser, R.S. Advances in the study of GPCRs by (19)F NMR. Curr. Opin. Struct. Biol. 2021, 69, 169–176.
7. Hilger, D.; Masureel, M.; Kobilka, B.K. Structure and dynamics of GPCR signaling complexes. Nat. Struct. Mol. Biol. 2018, 25, 4–12.
8. Huang, S.K.; Pandey, A.; Tran, D.P.; Villanueva, N.L.; Kitao, A.; Sunahara, R.K.; Sljoka, A.; Prosser, R.P. Delineating the conformational landscape of the adenosine A2A receptor during G protein coupling. Cell 2021, 184, 1884–1894.e14.
9. Sljoka, A. Probing Allosteric Mechanism with Long-Range Rigidity Transmission Across Protein Networks. Methods Mol. Biol. 2021, 2253, 61–75.
10. Di Pietrantonio, C.; Pandey, A.; Gould, J.; Hasabins, A.; Prosser, R.S. Understanding Protein Function Through an Ensemble Description: Characterization of Functional States by (19)F NMR. Methods Enzymol. 2019, 615, 103–130.
11. Huang, Y.; Wang, X.; Lv, G.; Razavi, A.M.; Huysmans, G.H.M.; Weinstein, H.; Bracken, C.; Eliezer, D.; Boudker, O. Use of paramagnetic (19)F NMR to monitor domain movement in a glutamate transporter homolog. Nat. Chem. Biol. 2020, 16, 1006–1012.

12. Meiboom, S.; Gill, D. Modified SpinEcho Method for Measuring Nuclear Relaxation Times. Rev. Sci. Instrum. 1958, 28, 688–691.
13. Zhuravleva, A.; Korzhnev, D.M. Protein folding by NMR. Prog. Nucl. Magn. Reson. Spectrosc. 2017, 100, 52–77.
14. Manglik, A.; Kim, T.H.; Masureel, M.; Altenbach, C.; Yang, Z.; Hilger, D.; Lerch, M.T.; Kobilka, T.S.; Thian, F.S.; Hubbell, W.L.; et al. Structural Insights into the Dynamic Process. of beta2-Adrenergic Receptor Signaling. Cell 2015, 161, 1101–1111.
15. Boeszoermenyi, A.; Chhabra, S.; Dubey, A.; Radeva, D.L.; Burdzhiev, N.T.; Chanev, C.D.; Petrov, O.I.; Gelev, V.M.; Zhang, M.; Anklin, C.; et al. Aromatic (19)F-(13)C TROSY: A background-free approach to probe biomolecular structure, function, and dynamics. Nat. Methods 2019, 16, 333–340.
16. Cellitti, S.E.; Jones, D.H.; Lagpacan, L.; Hao, X.; Zhang, Q.; Hu, H.; Brittain, S.M.; Brinker, A.; Caldwell, J.; Bursulaya, B.; et al. In vivo incorporation of unnatural amino acids to probe structure, dynamics, and ligand binding in a large protein by nuclear magnetic resonance spectroscopy. J. Am. Chem. Soc. 2008, 130, 9268–9281.
17. Didenko, T.; Liu, J.J.; Horst, R.; Stevens, R.C.; Wüthrich, K. Fluorine-19 NMR of integral membrane proteins illustrated with studies of GPCRs. Curr. Opin. Struct. Biol. 2013, 23, 740–747.
18. Yang, F.; Yu, X.; Liu, C.; Qu, C.-X.; Gong, Z.; Liu, H.-D.; Li, F.-H.; Wang, H.-M.; He, D.-F.; Yi, F.; et al. Phospho-selective mechanisms of arrestin conformations and functions revealed by unnatural amino acid incorporation and (19)F-NMR. Nat. Commun. 2015, 6, 8202.
19. Kuhlbrandt, W. Biochemistry. The resolution revolution. Science 2014, 343, 1443–1444.
20. Hite, R.K.; MacKinnon, R. Structural Titration of Slo2.2, a Na+-Dependent K+ Channel. Cell 2017, 168, 390–399.e11.
21. Liao, M.; Cao, E.; Julius, D.; Cheng, Y. Structure of the TRPV1 ion channel determined by electron cryo-microscopy. Nature 2013, 504, 107–112.
22. Cao, E.; Liao, M.; Cheng, Y.; Julius, Y. TRPV1 structures in distinct conformations reveal activation mechanisms. Nature 2013, 504, 113–118.
23. Paulsen, C.E.; Armache, J.P.; Gao, Y.; Cheng, Y.; Julius, D. Structure of the TRPA1 ion channel suggests regulatory mechanisms. Nature 2015, 525, 552.
24. Jin, P.; Bulkley, D.; Guo, Y.; Zhang, W.; Guo, Z.; Huynh, W.; Wu, S.; Meltzer, S.; Cheng, T.; Jan, L.Y.; et al. Electron. cryo-microscopy structure of the mechanotransduction channel NOMPC. Nature 2017, 547, 118–122.
25. Hirschi, M.; Herzik, M.A., Jr.; Wie, J.; Suo, Y.; Borschel, W.F.; Ren, D.; Lander, G.C.; Lee, S.-Y. Cryo-electron microscopy structure of the lysosomal calcium-permeable channel TRPML3. Nature

2017, 550, 411–414.

26. Chen, Q.; She, J.; Zeng, W.; Guo, J.; Xu, H.; Bai, X.C.; Jiang, Y. Structure of mammalian endolysosomal TRPML1 channel in nanodiscs. Nature 2017, 550, 415–418.
27. Zhang, K.; Julius, D.; Cheng, Y. Structural snapshots of TRPV1 reveal mechanism of polymodal functionality. Cell 2021, 184, 5138–5150.e12.
28. Steinberg, X.; Kasimova, M.A.; Cabezas-Bratesco, D.; Galpin, J.D.; Ladron-de-Guevara, E.; Villa, F.; Carnevale, V.; Islas, L.; Ahern, C.A.; Brauchi, S.E. Conformational dynamics in TRPV1 channels reported by an encoded coumarin amino acid. eLife 2017, 6, e28626.
29. Chen, I.; Pant, S.; Wu, Q.; Cater, R.J.; Sobti, M.; Vandenberg, R.J.; Stewart, A.G.; Tajkhorshid, E.; Font, J.; Ryan, R.M. Glutamate transporters have a chloride channel with two hydrophobic gates. Nature 2021, 591, 327–331.
30. Cater, R.J.; Ryan, R.M.; Vandenberg, R.J. The Split Personality of Glutamate Transporters: A Chloride Channel and a Transporter. Neurochem. Res. 2016, 41, 593–599.
31. Arkhipova, V.; Guskov, A.; Slotboom, D.J. Structural ensemble of a glutamate transporter homologue in lipid nanodisc environment. Nat. Commun. 2020, 11, 998.
32. Ge, J.; Elferich, J.; Dehghani-Ghahnaviyeh, S.; Zhao, Z.; Meadows, M.; von Gersdorff, H.; Tajkhorshid, E.; Gouaux, E. Molecular mechanism of prestin electromotive signal amplification. Cell 2021, 184, 4669–4679.e13.
33. Bavi, N.; Clark, M.D.; Contreras, G.F.; Shen, R.; Reddy, B.G.; Milewski, W.; Perozo, E. The conformational cycle of prestin underlies outer-hair cell electromotility. Nature 2021, 600, 553–558.
34. Butan, C.; Song, Q.; Bai, J.-P.; Tan, W.J.Y.; Navaratnam, D.; Santos-Sacchi, J. Single particle cryo-EM structure of the outer hair cell motor protein prestin. Nat. Commun. 2022, 13, 290.
35. Santos-Sacchi, J.; Shen, W.; Zheng, J.; Dallos, P. Effects of membrane potential and tension on prestin, the outer hair cell lateral membrane motor protein. J. Physiol. 2001, 531, 661–666.
36. Schumacher, S.; Deddebm, D.; Nunez, R.V.; Matoba, K.; Takagi, J.; Biertümpfel, C.; Mizuno, N. Structural insights into integrin alpha5beta1 opening by fibronectin ligand. Sci. Adv. 2021, 7, eabe9716.
37. Klebl, D.P.; White, H.D.; Sobott, F.; Muench, S.P. On-grid and in-flow mixing for time-resolved cryo-EM. Acta Crystallogr. D Struct. Biol. 2021, 77, 1233–1240.
38. Kaledhonkar, S.; Fu, Z.; White, H.; Frank, J. Time-Resolved Cryo-electron Microscopy Using a Microfluidic Chip. Methods Mol. Biol. 2018, 1764, 59–71.

39. Maeots, M.E.; Lee, B.; Nans, A.; Jeong, S.-G.; Esfahani, M.M.N.; Ding, S.; Smith, D.J.; Lee, C.-S.; Lee, S.S.; Peter, M.; et al. Modular microfluidics enables kinetic insight from time-resolved cryo-EM. Nat. Commun. 2020, 11, 3465.

40. Dandey, V.P.; Budell, W.C.; Wei, H.; Bobe, D.; Maruthi, K.; Kopylov, M.; Eng, E.T.; Kahn, P.A.; Hinshaw, J.E.; Kundu, N.; et al. Time-resolved cryo-EM using Spotiton. Nat. Methods 2020, 17, 897–900.

41. Shaikh, T.R.; Barnard, D.; Meng, X.; Wagenknecht, T. Implementation of a flash-photolysis system for time-resolved cryo-electron microscopy. J. Struct. Biol. 2009, 165, 184–189.

42. Yoder, N.; Jalali-Yazdi, F.; Noreng, S.; Houser, A.; Baconguis, I.; Gouaux, E. Light-coupled cryo-plunger for time-resolved cryo-EM. J. Struct. Biol. 2020, 212, 107624.

43. Weinert, T.; Skopintsev, P.; James, D.; Dworkowski, F.; Panepucci, E.; Kekilli, D.; Furrer, A.; Brünle, S.; Mous, S.; Ozerov, D.; et al. Proton uptake mechanism in bacteriorhodopsin captured by serial synchrotron crystallography. Science 2019, 365, 61–65.

44. Martin-Garcia, J.M. Protein Dynamics and Time Resolved Protein Crystallography at Synchrotron Radiation Sources: Past, Present and Future. Crystals 2021, 11, 521.

45. Wickstrand, C.; Nogly, P.; Nango, E.; Iwata, S.; Standfuss, J.; Neutze, R. Bacteriorhodopsin: Structural Insights Revealed Using X-ray Lasers and Synchrotron Radiation. Annu. Rev. Biochem. 2019, 88, 59–83.

46. Baxter, R.H.; Ponomarenko, N.; Srajer, V.; Pahl, R.; Moffat, K.; Norris, J.R. Time-resolved crystallographic studies of light-induced structural changes in the photosynthetic reaction center. Proc. Natl. Acad. Sci. USA 2004, 101, 5982–5987.

47. Wohri, A.B.; Katona, G.; Johansson, L.C.; Fritz, E.; Malmerberg, E.; Andersson, M.; Vincent, J.; Eklund, M.; Cammarata, M.; Wulff, M.; et al. Light-induced structural changes in a photosynthetic reaction center caught by Laue diffraction. Science 2010, 328, 630–633.

48. Neutze, R.; Wouts, R.; van der Spoel, D.; Weckert, E.; Hajdu, J. Potential for biomolecular imaging with femtosecond X-ray pulses. Nature 2000, 406, 752–757.

49. Aquila, A.; Hunter, M.S.; Doak, R.B.; Kirian, R.A.; Fromme, P.; White, T.A.; Andreasson, J.; Arnlund, D.; Bajt, S.; Barends, T.R.M.; et al. Time-resolved protein nanocrystallography using an X-ray free-electron laser. Opt. Express 2012, 20, 2706–2716.

50. Kern, J.; Alonso-Mori, R.; Tran, R.; Hattne, J.; Gildea, R.J.; Echols, N.; Glöckner, C.; Hellmich, J.; Laksmono, H.; Sierra, R.G.; et al. Simultaneous femtosecond X-ray spectroscopy and diffraction of photosystem II at room temperature. Science 2013, 340, 491–495.

51. Kupitz, C.; Basu, S.; Grotjohann, I.; Fromme, R.; Zatsepin, N.A.; Rendek, K.N.; Hunter, M.S.; Shoeman, R.L.; White, T.A.; Wang, D.; et al. Serial time-resolved crystallography of photosystem

II using a femtosecond X-ray laser. Nature 2014, 513, 261–265.

52. Kern, J.; Tran, R.; Alonso-Mori, R.; Koroidov, S.; Echols, N.; Hattne, J.; Ibrahim, M.; Gul, S.; Laksmono, H.; Sierra, R.G.; et al. Taking snapshots of photosynthetic water oxidation using femtosecond X-ray diffraction and spectroscopy. Nat. Commun. 2014, 5, 4371.
53. Suga, M.; Akita, F.; Hirata, K.; Ueno, G.; Murakami, H.; Nakajima, Y.; Shimizu, T.; Yamashita, K.; Yamamoto, M.; Ago, H.; et al. Native structure of photosystem II at 1.95 A resolution viewed by femtosecond X-ray pulses. Nature 2015, 517, 99–103.
54. Young, I.D.; Ibrahim, M.; Chatterjee, R.; Gul, S.; Fuller, F.; Koroidov, S.; Brewster, A.S.; Tran, R.; Alonso-Mori, R.; Kroll, T.; et al. Structure of photosystem II and substrate binding at room temperature. Nature 2016, 540, 453–457.
55. Sauter, N.K.; Echols, N.; Adams, P.D.; Zwart, P.H.; Kern, J.; Brewster, A.S.; Koroidov, S.; Alonso-Mori, R.; Zouni, A.; Messinger, J.; et al. No observable conformational changes in PSII. Nature 2016, 533, E1–E2.
56. Suga, M.; Akita, F.; Sugahara, M.; Kubo, M.; Nakajima, Y.; Nakane, T.; Yamashita, K.; Umena, Y.; Nakabayashi, M.; Yamane, T.; et al. Light-induced structural changes and the site of O = O bond formation in PSII caught by XFEL. Nature 2017, 543, 131–135.
57. Kern, J.; Chatterjee, R.; Young, I.D.; Fuller, F.D.; Lassalle, L.; Ibrahim, M.; Gul, S.; Fransson, T.; Brewster, A.S.; Alonso-Mori, R.; et al. Structures of the intermediates of Kok's photosynthetic water oxidation clock. Nature 2018, 563, 421–425.
58. Suga, M.; Akita, F.; Yamashita, K.; Nakajima, Y.; Ueno, G.; Li, H.; Yamane, T.; Hirata, K.; Umena, Y.; Yonekura, S.; et al. An oxyl/oxo mechanism for oxygen-oxygen coupling in PSII revealed by an X-ray free-electron laser. Science 2019, 366, 334–338.
59. Ibrahim, M.; Fransson, T.; Chatterjee, R.; Cheah, M.H.; Hussein, R.; Lassalle, L.; Sutherlin, K.D.; Young, I.D.; Fuller, F.D.; Gul, S.; et al. Untangling the sequence of events during the S2 --> S3 transition in photosystem II and implications for the water oxidation mechanism. Proc. Natl. Acad. Sci. USA 2020, 117, 12624–12635.
60. Hussein, R.; Ibrahim, M.; Bhowmick, A.; Simon, P.S.; Chatterjee, R.; Lassalle, L.; Doyle, M.; Bogacz, I.; Kim, I.-S.; Cheah, M.H.; et al. Structural dynamics in the water and proton channels of photosystem II during the S2 to S3 transition. Nat. Commun. 2021, 12, 6531.
61. Bao, H.; Burnap, R.L. Photoactivation: The Light-Driven Assembly of the Water Oxidation Complex. of Photosystem II. Front. Plant Sci. 2016, 7, 578.
62. Kok, B.; Forbush, B.; McGloin, M. Cooperation of charges in photosynthetic O2 evolution-I. A linear four step mechanism. Photochem. Photobiol. 1970, 11, 457–475.

63. Dods, R.; Båth, P.; Morozov, D.; Gagnér, V.A.; Arnlund, D.; Luk, H.L.; Kübel, J.; Maj, M.; Vallejos, A.; Wickstrand, C.; et al. Ultrafast structural changes within a photosynthetic reaction centre. Nature 2021, 589, 310–314.

64. Lanyi, J.K. Bacteriorhodopsin. Annu. Rev. Physiol. 2004, 66, 665–688.

65. Nango, E.; Royant, A.; Kubo, M.; Nakane, T.; Wickstrand, C.; Kimura, T.; Tanaka, T.; Tono, K.; Song, C.; Tanaka, R.; et al. A three-dimensional movie of structural changes in bacteriorhodopsin. Science 2016, 354, 1552–1557.

66. Nogly, P.; Weinert, T.; James, D.; Carbajo, S.; Ozerov, D.; Furrer, A.; Gashi, D.; Borin, V.; Skopintsev, P.; Jaeger, K.; et al. Retinal isomerization in bacteriorhodopsin captured by a femtosecond X-ray laser. Science 2018, 361, eaat0094.

67. Kovacs, G.N.; Colletier, J.P.; Grünbein, M.L.; Yang, Y.; Stensitzki, T.; Batyuk, A.; Carbajo, S.; Doak, R.B.; Ehrenberg, D.; Foucar, L.; et al. Three-dimensional view of ultrafast dynamics in photoexcited bacteriorhodopsin. Nat. Commun. 2019, 10, 3177.

68. Skopintsev, P.; Ehrenberg, D.; Weinert, T.; James, D.; Kar, R.K.; Johnson, P.J.M.; Ozerov, D.; Furrer, A.; Martiel, I.; Dworkowski, F.; et al. Femtosecond-to-millisecond structural changes in a light-driven sodium pump. Nature 2020, 583, 314–318.

69. Yun, J.H.; Li, X.; Yue, J.; Park, J.-H.; Jin, Z.; Li, C.; Hu, H.; Shim, Y.; Pandey, S.; Carbajo, S.; et al. Early-stage dynamics of chloride ion-pumping rhodopsin revealed by a femtosecond X-ray laser. Proc. Natl. Acad. Sci. USA 2021, 118, e2020486118.

70. Oda, K.; Nomura, T.; Nakane, T.; Yamashita, K.; Inoue, K.; Ito, S.; Vierock, J.; Hirata, K.; Maturana, A.D.; Katayama, K.; et al. Time-resolved serial femtosecond crystallography reveals early structural changes in channelrhodopsin. eLife 2021, 10, e62389.

71. Shimada, A.; Kubo, M.; Baba, S.; Yamashita, K.; Hirata, K.; Ueno, G.; Nomura, T.; Kimura, T.; Shinzawa-Itoh, K.; Baba, J.; et al. A nanosecond time-resolved XFEL analysis of structural changes associated with CO release from cytochrome c oxidase. Sci. Adv. 2017, 3, e1603042.

72. Ishigami, I.; Lewis-Ballester, A.; Echelmeier, A.; Brehm, G.; Zatsepin, N.A.; Grant, T.D.; Coe, J.D.; Lisova, S.; Nelson, G.; Zhang, S.; et al. Snapshot of an oxygen intermediate in the catalytic reaction of cytochrome c oxidase. Proc. Natl. Acad. Sci. USA 2019, 116, 3572–3577.

73. Gisriel, C.; Coe, J.; Letrun, R.; Yefanov, O.M.; Luna-Chavez, C.; Stander, N.E.; Lisova, S.; Mariani, V.; Kuhn, M.; Aplin, S.; et al. Membrane protein megahertz crystallography at the European XFEL. Nat. Commun. 2019, 10, 5021.